Proceedings of the 8th World Congress on Civil, Structural, and Environmental Engineering (CSEE'23)
Lisbon, Portugal – March 29 – 31, 2023
Paper No. ICGRE 115
DOI: 10.11159/icgre23.115

Mechanical Response of Tailings under Monotonic Triaxial Tests in Unsaturated and Nearly Saturated Conditions

Gianluca Bella
Pini Group Ltd
Via Besso 7, Lugano, Switzerland
gianluca.bella@pini.group

Abstract - A detailed knowledge of the mechanical behaviour of unsaturated tailing wastes is a key element to assess the stability analysis of tailing facilities, considering the variation of the soil strength due to climate effects, rainfall, or poor management in order to minimize the high rate of recent failures associated with unacceptable fatalities, economic and environmental damages. This research investigates the mechanical behaviour of unsaturated fluorite ore wastes collected after the failure of the Stava tailing dams (Italy). The static liquefaction response of the tailings was studied by carrying out CIU triaxial tests by through application of different backpressures to obtain unsaturated or nearly saturated specimens. The influence of the degree of saturation on the mechanical response of Stava tailings is investigated and the static liquefaction strength evaluated. Outcomes are interpreted based on the Water Retention Curve estimated by performing water retention tests on the same soil, and within the Critical State framework. Results are also compared with those obtained in fully saturated conditions from a previous experimental campaign.

Keywords: tailings; triaxial test; unsaturated soil; Critical State Parameter; Water Retention Curve; Stava.

1. Introduction

Mines build tailing dams (TSF) to safely store tailing wastes having the consistence of a slurry, paste cake or paste. TSF are complex geotechnical structures subjected to many interactions with the atmosphere that govern the position of the water table within the basin, leading to variations in the height of the unsaturated zone above the phreatic surface. Their performance need to be assessed both during mining and after operations cease, and any combination of improper design, construction and management could result in failures, as highlighted by the high rate of recent collapses that caused fatalities, economic and environmental damages ([1]-[2]). Defined as a temporary loss of the shear strength of saturated loose soils when the pore water pressure became the same of normal stress, the static liquefaction is a consequence of intense rainfall or rapid snowmelt associated to poor management and represents one of the main causes of 25% of tailing dams collapses recorded since the early twentieth century ([3] and Fig. 1). Fast dam rise, seepage/piping, wrong design choices, dynamic liquefaction, overtopping, and foundation failures represent additional causes of collapse (Tab. 1).

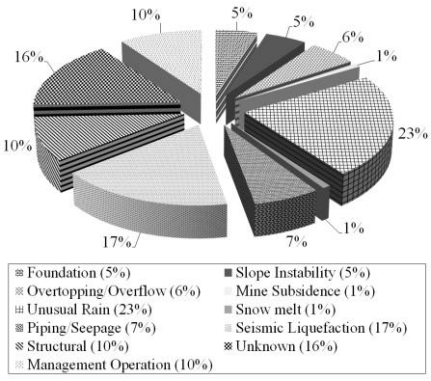

Fig. 1: Distribution of the number of failures and causes in the world (modified from [4]).

Table 1: List of the main tailings dam breaches occurred in the last four decades, causes, fatalities and reference (modified from [5]).

Incident	Year	Failure mode	Casualty	Ref.
Stava (Italy)	1985	Cascade collapse of two dams triggered static liquefaction	268	[6]
Merriespruit (South Africa)	1997	Overtopping and slope failure	17	[7]
Kolontár (Hungary)	2010	Piping failure	10	[8]
Mount Polley (Canada)	2014	Foundation and overtopping failure	0	[9]
Mariana (Brazil)	2015	Earthquake triggered static liquefaction	19	[10]
Cadia (Australia)	2018	Foundation failure	0	[11]
Brumadinho (Brazil)	2019	Collapse due to static liquefaction	270	[12]

Moving from these reasons, this study gives the main overcome of an experimental campaign to investigate the mechanical behaviour of Stava silty tailings. The static liquefaction response is investigated by carrying out monotonic triaxial tests on silty sample under unsaturated and nearly saturated conditions. The role of the saturation state is investigated, and the static liquefaction strength is evaluated. Results are interpreted within the Critical State framework, my means water retention curves (WRC) and outcomes from a previous experimental campaign on the same soul under fully saturated conditions.

2. Testing material and experimental apparatus

The mechanical response of Stava tailings was studied by means of an experimental campaign carried out at Politecnico di Torino (Italy) on unsaturated and nearly saturated tailing samples. Stava tailings were collected from the lower portion of the upper embankment which remained in place after the collapse occurred in 1985. Built one above the other on a natural slope near the city of Stava, the two tailing dams were aimed to store the waste products resulting from the mining activities of Prestavel fluorite plants. The collapse of the upper dam on the lower basin triggered a $250 \cdot 10^3$ m^3 flow-slide that crossed the Stava valley at a speed of 90 km/h, leading to 268 fatalities, with relevant economic and environmental damages. A poor drainage, the high phreatic level and the unconsolidated state of tailings were supposed to be the main factors that caused the static liquefaction, leading the collapse of the Stava dams. Tailings used in the current research consist of the silt fraction passing through a sieve n°200 (grain seize distribution in Fig. 2), and represent the fraction deposited into Stava basins. The liquid limit is w_L=27.4%, the plastic limit was evaluated w_P=18.0% and the plasticity index was PI=9.4 ([13]-[14]), with a specific gravity equal G_S=2.828 and hydraulic conductivity k=10^{-7}m/s. X-ray diffraction analysis allowed to show a significant amount of calcite and fluorite ([15]-[16]).

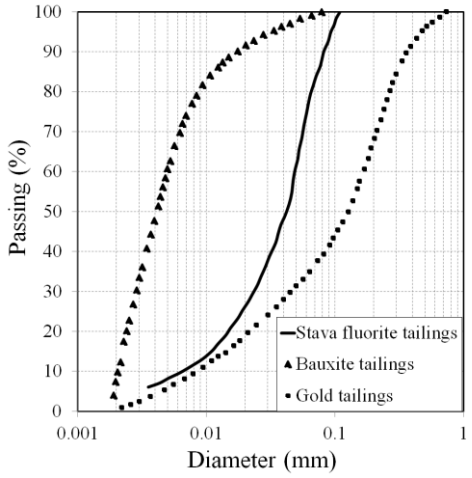

Fig. 2: Grain size distribution of the Stava silty fraction and comparison with other tailings (modified from [17]).

Table 2: Initial state of Stava samples. void ratio (e_0), water content (w_0), dry unit weight (γ_d), B-Skempton parameter (B). State of the Stava samples at the end of the consolidation phase: void ratio (e_C), degree of saturation (Sr_C), and comments.

Sample	e_0 (-)	w_0 (-)	γ_d (kN/m^3)	B (-)	e_c (-)	Sr_c (%)	Com-ments*
TXT_1	1.22	5.0	12.75	0.99	0.82	98.1	L.
TXT_2	1.23	5.0	12.65	0.98	0.84	97.2	L.
TXT_3	1.20	5.0	12.85	0.97	0.71	98.5	L.
TXT_4	1.25	5.0	12.59	0.96	0.79	97.0	L.
TXT_5	1.34	5.0	12.07	0.91	0.78	88.9	N.L.
TXT_6	1.20	5.0	12.85	0.89	0.75	97.3	L.

*L.=liquefied, N.L.=not liquefied.

The static liquefaction response was investigated by means of monotonic triaxial tests carried out on samples 38 mm initial diameter and 76 mm initial height. The moist tamping technique was used to compact all the samples inside the conventional Bishop and Wesley's cell to reproduce the deposition techniques of Stava tailing wastes inside the basins. Details can be found in [6], and the list of performed triaxial tests is given in Table 2. Each triaxial test consisted of:

- saturation. It consisted of upward flushing with de-aired water, followed by back pressuring performed step-by-step (drainages are closed), by increasing the confining pressure $\Delta\sigma_3$ and then measuring the change in pore pressure Δu, and so evaluating the saturation level by means of the -B Skempton parameter B= $\Delta u/\Delta\sigma_3$. The entire

procedure was then repeated for different B-values, leading sample in unsaturated conditions (B<0.97) or nearly saturated conditions (B≥0.97);
- consolidation. Performed under drained conditions, it was carried out to achieve a desired effective stress approx. 80 kPa (isotropic conditions);
- shearing. It was carried out in undrained conditions at constant radial effective stress (strain-controlled conditions). Finally, the specimen was extracted from the cell and weighted. After being oven dried for 24 hours at 105°C, the specimen was weighted to obtain the water content at the end of the isotropic consolidation, assuming no variations of water content during the undrained shearing phase.

Outcomes have been interpreted throughout the experimental results of triaxial tests in fully saturated conditions ([13]-[14]), or in unsaturated conditions based on the WRC obtained by performing water retention tests ([18]-[2]) and suction-controlled triaxial tests ([19]). Details are given in [6].

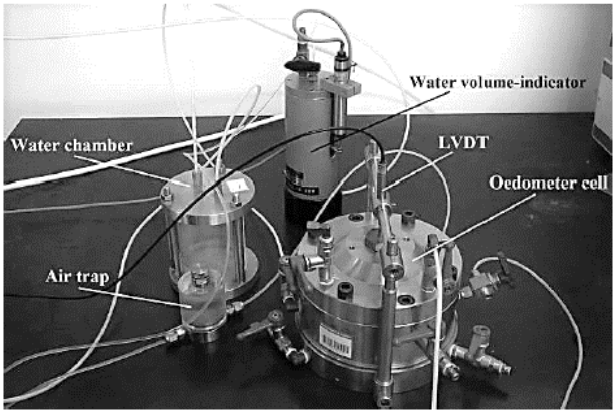

Fig. 3: Suction-controlled oedometer: main components ([2]).

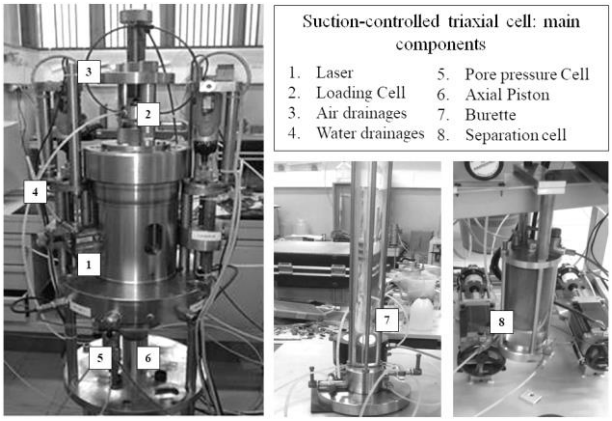

Fig. 4: Suction-controlled triaxial cell: main components ([19]).

3. Experimental results

In Section 3.1, the mechanical response of Stava tailings in unsaturated and nearly saturated conditions is shown and the role of the degree of saturation is investigated in terms of shear strength resistance. In Section 3.2 a preliminary interpretation of the mechanical behaviour is given within the Critical State framework, also accounting for the outcomes of previous experimental campaigns under fully saturated conditions, and under unsaturated conditions in terms of water retention curves.

3.1 Influence of the degree of saturation and evaluation of the static liquefaction strength of Stava tailings

The effect of degree of saturation on the stress-strain response of Stava tailings is shown in Fig. 5. The void ratio at the end of the consolidation phase ranged between 0.84 and 0.75 for all samples, except for tests TXT_3 which exhibited the same tendency to liquefy as all other samples, with the only exception of TXT_5. This suggested that, upon certain values, the initial density has not a significant effect on the mechanical behaviour of Stava tailings. Otherwise, TXT_5 was the only specimen having a degree of saturation less than 90% and it was the only specimen to exhibit a hardening behaviour.

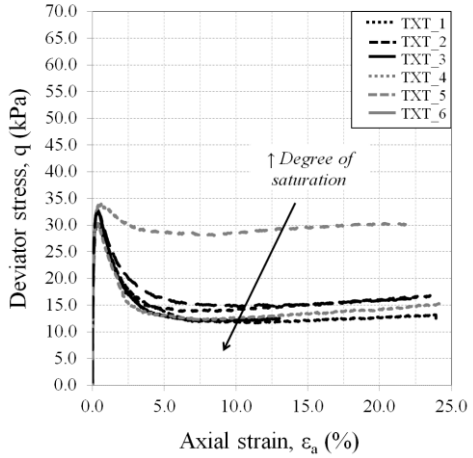

Fig. 5: Influence of the degree of saturation on the mechanical behaviour of Stava tailings: stress-strain curves (all samples).

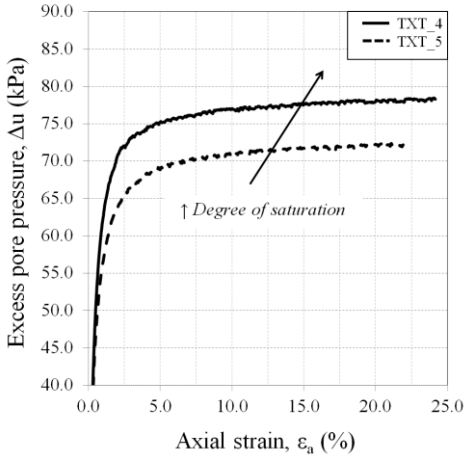

Fig. 6: Effect of the degree of saturation on the excess of pore pressure for samples TXT_4 and TXT_5.

The importance of the degree of saturation in determining the soil response can be observed by analysing tests TXT_4 and TXT_5. The two samples have the same initial void ratio (e_c=0.79 TXT_4, and e_c=0.78 TXT_5) but different degree of saturation (Sr_c=97%TXT_4, and Sr_c=89% TXT_5), so that the first one exhibits a softening response with higher excess of pore pressure (Δu=79 kPa) if compared with the excess of pore pressure of the second sample (Δu=71 kPa) that is characterized by an hardening response (Fig. 6). According to [20], the equation proposed by [21] for cyclic loading conditions can be generalized to evaluate the liquefaction resistance under monotonic loading conditions, giving the liquefaction resistance ratio LRR depending on the degree of saturation (Eq.(1a)):

$$LRR = \log(\alpha \cdot \varepsilon_v^* + 10) \quad \text{with} \quad \varepsilon_v^* = \frac{p_c'}{p_0 + p_c'} \cdot (1 - Sr) \cdot \frac{e}{1+e} \tag{1a, 1b}$$

where α is a parameter to be calibrated, ε_{v^*} is the potential volumetric strain (Eq.(1b)) evaluated by knowledge of the pore water pressure (p_0), the mean effective confinement stress (p'_C), and the void ratio. The liquefaction resistance of unsaturated specimen TXT_5 (Sr_c=89%) is more than 2 times greater than that of nearly saturated samples TXT_1→TXT_4, TXT_6 (Sr_c≥97%), as shown in Fig. 7.

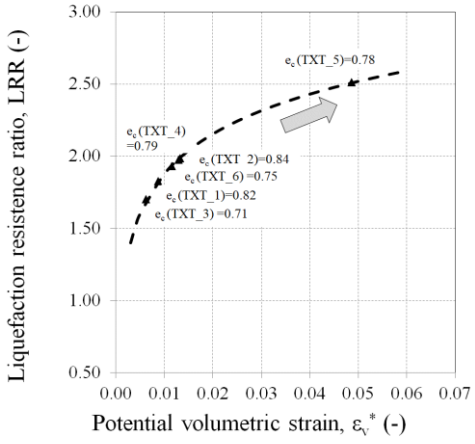

Fig. 7: LRR with the potential volumetric strain.

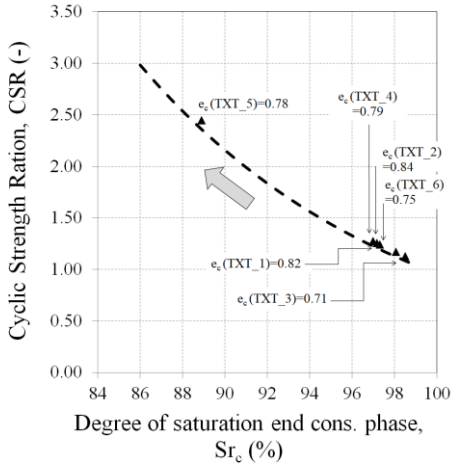

Fig. 8: CSR with the degree of saturation.

According to [20], another equation can be adopted to evaluate the static liquefaction resistance at different degrees of saturation. This equation, proposed by [22] for cyclic loading conditions, gives an exponential relationship between the liquefaction resistance and the B-value:

$$(CSR)_{uns} = (CSR)_{sat} \cdot 10^{[\beta(1-B)]} \quad (2)$$

where CSR_{uns} is the cyclic strength stress ratio under unsaturated conditions, CSR_{sat} is the cyclic strength stress ratio under fully saturated conditions, B is the Skempton parameter and β is a parameter to be calibrated. In the current research, the cyclic strength stress ratio under fully saturated conditions is assumed equal to one and Eq.(2) was applied by assuming B≈Sr. Also in this case, the liquefaction strength of unsaturated specimen is proved to be more than 2 times greater than that of nearly saturated samples (Fig. 8). Finally, according to [23], the residual strength was estimated by knowledge of the residual deviator stress and the friction angle (Eq.(3)):

$$S_{us} = \frac{1}{2} \cdot q_{res} \cdot \cos(\varphi_{cv}) \quad (3)$$

The residual deviatoric stress was given by Fig.5, while the friction angle (φ_{cv}=33°) was estimated by previous works ([6]-[13]). Results are given in Tab. 3 and are in good agreement with those previously shown in Fig. 7 and Fig. 8.

Table 3: Degree of saturation (Sr_c) at the end of the consolidation phase, residual deviatoric stress (q_{res}), and residual strength (S_{us}).

Sample	Sr_c (%)	q_{res} (kPa)	Su (kPa)
TXT_1	98.1	12.6	5.0
TXT_2	97.2	16.6	7.0
TXT_3	98.5	12.5	4.5
TXT_4	97.0	15.3	6.3
TXT_5	88.9	29.0	12.5
TXT_6	97.3	16.4	6.8

3.2 Critical State theory: a preliminary interpretation of the mechanical response of Stava tailings

The tendency of a granular soil to liquefy or not was defined by [24] based on the state parameter ψ. The Authors defined the state parameters as the difference between the initial void ratio and the void ratio at Critical State (Eq.(4)):

$$\psi = e - e_{cs} \quad (4)$$

In the compression plane, a positive state parameter is related to loose specimen susceptible to liquefaction, while a negative state parameter deals with an initial state of the sample lying below the Critical State Line (CSL) and it is related to dense specimen no susceptible to liquefaction (hardening response). The final conditions for triaxial tests in saturated conditions are given in terms of void ratio and mean effective stress. The red circles represent the final state of saturated samples ([13]): provided in terms of void ratio and mean Bishop effective stress ($p'_B = p_{net} + \chi \cdot s$, assuming χ=Sr), they are connected by a soild line that represents the CSL of Stava silt specimen in saturated conditions (suction 0kPa). The squares represent the final state of unsaturated samples obtained in a previous experimental campaign by means of suction-controlled triaxial test: they are connected by a dotted line that represents the iso-suction Critical State Line (suction approx. 30/40kPa) of the unsaturated Stava silt specimen ([6]). The two experimental data set, in saturated conditions and unsaturated conditions, lie in a narrow area so the CSL for unsaturated samples is quite close to the CSL for saturated samples, increasing its slope at high stress values, as shown in Fig. 9. In the same plane, the initial state of samples tested in the current research is given by the black circles (nearly saturated samples: TXT_1→TXT_4, TXT_6) and the empty triangle (unsaturated sample: TXT_5).

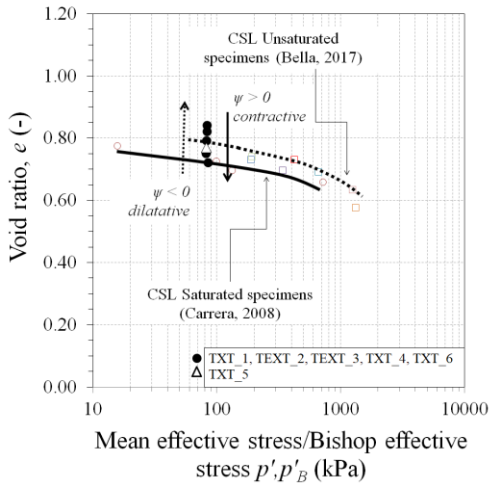

Fig. 9: CSL for saturated and unsaturated silt specimens.

Table 4 Gallipoli water retention parameters n, m, Φ and ψ for Stava silty samples (main drying branch and main wetting branch).

Main drying branch			
n (-)	m (-)	Φ (kPa^{-1})	ψ (-)
1.670	0.400	0.281	5.327

Main wetting branch			
n (-)	m (-)	Φ (kPa^{-1})	ψ (-)
1.500	0.330	5.405	7.810

It can be observed that all initial states of nearly saturated samples lie above the CLS related to saturated conditions, so a contractive behaviour is expected. On the other hand, the initial state of the unsaturated sample TXT_5 lies below the CLS related to unsaturated conditions, so a hardening response is expected. The suction levels reached by samples were estimated from the WRC associated with the void ratio reached at the end of the consolidation phase. They are evaluated by using the model proposed by [25] (Eq.(5)), allowing to estimate the evolution of the water retention response with void ratio (n, m, ψ, Φ soil parameters are summarized in Tab. 4).

$$Sr = 1/(1 + [\phi(v-1)^{\psi} s]^{n})^{m} \quad (5)$$

A 3D representation of the WRC for Stava silty tailings is given in Fig. 10, and a section corresponding to e=0.78 is provided in Fig. 11. Knowledge of water ratio (e_w=Sr·e) allowed to estimate the suction level reached by sample TXT_4 and TXT_5 on the main drying/wetting branches. Suction associated to nearly saturated sample TXT_4 (Sr_c=97%) is almost null, while unsaturated sample TXT_5 (Sr_c=89%) is characterized by a suction ranging between 2kPa and 20kPa. With reference to the position of the initial state of unsaturated sample TXT_5 in the compression plane (Fig. 9), it well justifies the assumption that the empty triangle should be preliminary associated with the CSL for unsaturated specimens, giving a state parameter less than zero, and so resulting in a hardening behaviour (Fig. 5).

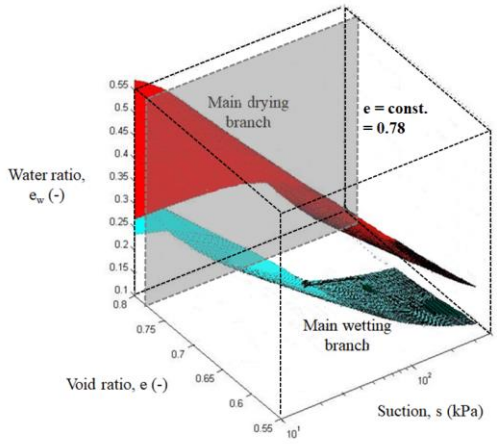

10)

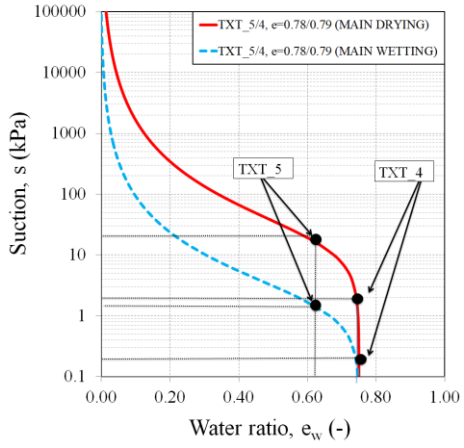

11)

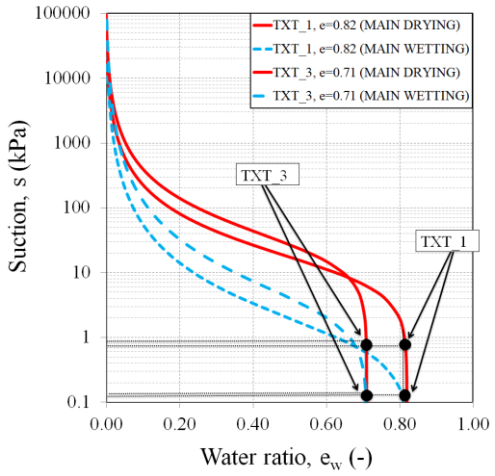

12)

Fig. 10: Three-dimensional representation of the WRC evaluated from water retention tests.

Fig. 11: Water retention curves of sample TXT_4 and TXT_5, evaluation of the suction level.

Fig. 12: Water retention curves of sample TXT_1 and TXT_3, evaluation of the suction level.

The suction levels associated to samples TXT_1 (Sr_c=98.1%), TXT_3 (Sr_c=98.5%) and TXT_4 (Sr_c=97%) are nearly null, as shown in Fig.11 and Fig.12. This well justifies the hypothesis that their initial state (solid black circles, Fig. 9) can be correlated with the Critical State Line for saturated specimens, giving a state parameter higher than zero, and so leading the contractive response that was realistically experienced.

4. Conclusion

The in-depth knowledge of the mechanical behaviour of tailing wastes finds its practical application as a key tool to reliably assess the stability of the tailing storage facilities. Partially saturated and nearly saturated silty tailings were characterized by means of triaxial tests. The importance of the degree of saturation on the static liquefaction response is investigated and the static liquefaction strength is evaluated. The static liquefaction response is interpretated within the Critical State Theory by means of the experimental results obtained in a previous campaign in saturated and unsaturated conditions, and by using the concept of the state parameters. Despite the small scatter between CSL in saturated and unsaturated conditions, the evaluation of the suction associated to the unsaturated sample TXT_5 and its initial state with respect to the unsaturated CSL, allowed a preliminary explanation of its tendency to dilate.

Acknowledgements

The Author wishes to thank Prof. G. Musso (Politecnico di Torino) for his valuable inputs while analyzing the experimental data. The Author also wishes to acknowledge Dr. A. Azizi, Dr. O. Pallara and Mr. G. Bianchi for their help during the laboratory tests presented in this work.

References

[1] A. Azizi, G. Bella and I. Farashchi, “Evaluation of the capability of critical state constitutive model to predict the collapse potential of loose sand”. *Int. Symposium on Geohazards and Geomechanics*, vol. 26, pp. 1-14, 2015.

[2] G. Bella, ”Water retention behaviour of tailings in unsaturated conditions”, *Geomechanics and Engineering, An Int'l Journal*, vol. 26, no. 02, pp. 117-132, 2021.

[3] G. Bella, “Evaluation of the Static Liquefaction Behaviour of Silty Tailings in Unsaturated Conditions”. *Proceedings of the 7th International Conference on Geotechnical Research and Engineering*, Online - April, 10-12, 2022.

[4] M. Rico, G. Benito, A.R. Salgueiro, A. Dıez-Herrero and H. Pereira, “Reported tailings dam failures - A review of the European incidents in the worldwide context”, *J. of Hazardous Materials*, vol. 152, no. 02, pp. 846-852, 2008.

[5] S. Liu and M. Henderson, “An Overview on Methodologies for Tailings Dam Breach Study”, *Proceedings of the Tailings and Mine Waste Conference*, Denver - Colorado, 2020.

[6] G. Bella, “Hydro-Mechanical Behaviour of tailings in Unsaturated Conditions”, *Ph.D. dissertation*, Dept. Struct. Build. and Geotech. Eng., Politecnico di Torino, Italy, 2017.
[7] F. Wagener, H. Craig, G. Blight, G. McPhail, A. Williams and J. Strydom, “The Merriespruit tailings dam failure - a review”, *Proceedings of the Conference on Tailings and Mine Waste*, Colorado State University, Fort Collins, 1998.
[8] G. Grenerczy and U. Wegmüller, “Persistent scatterer interferometry analysis of the embankment failure of a red mud reservoir using ENVISAT ASAR data”, *Natural Hazards*, vol. 59, pp. 1047, 2011.
[9] IEEIRP, Report on Mount Polley Tailings Storage Facility Breach, January 30, 2015.
[10] N. Morgenstern, S. Vick, C. Viotti and B. Watts, “Fundão Tailings Dam Review Panel: Report on the Immediate Causes of the Failure of the Fundão Dam”, August 25, 2016.
[11] M. Jefferies, N. Morgenstern, D. Van Zyl and J. Wates, “Report on NTSF Embankment Failure Cadia Valley Operations for Ashurst Australia”, April 17, 2019.
[12] P. Roberston, L. De Melo, D. Williams and G. Wilson, “Report of the Expert Panel on the Tech-nical Causes of the Failure of Feijão Dam I”, December 12, 2019.
[13] A. Carrera, “Mechanical behaviour of Stava tailings”, *Ph.D. dissertation*, Dept. Struct. Build. and Geotech. Eng., Politecnico di Torino, Italy, 2008.
[14] A. Carrera, M. Coop and R. Lancellotta, “Influence of grading on the mechanical behaviour of Stava tailings”, *Géotechnique*, vol. 61, no. 11, pp. 935-946, 2011.
[15] G. Bella, F.S. Lameiras, T. Esposito, M. Barbero and F. Barpi, ”Aging Simulation of the Tailings from Stava Fluorite Extraction by Exposure to Gamma Rays”, *Revista Escola de Minas*, vol. 70, no. 04, pp. 483-490, 2017.
[16] G. Bella, M. Barbero, F. Lameiras, T. Esposito and F. Barpi, “Chemical-Physical Characterization of Stava Tailings Subjected to an Innovative Aging Technique”, *Proceedings of the 7th Int. Conference on Geotechnical Research and Engineering*, Online - April, 10-12, 2022.
[17] R. Sarsby, Environmental Geotechnics, ICE Publishing, 2013.
[18] G. Bella, “A Preliminary Insight into the Water Retention Response of Sand-Silt Mixtures of Stava Tailings”. *Proceedings of the 7th Int. Conference on Geotechnical Research and Engineering*, Online - April, 10-12, 2022.
[19] G. Bella and G. Musso, “Hydro-Mechanical Behaviour and Critical State Conditions of Unsaturated Silty Tailings”. *Proceedings of the 8th Int. Conference on Geotechnical Research and Engineering*, Lisbon - March, 29-31, 2023.
[20] J. He, J. Chu and H. Liu, “Undrained shear strength of desaturated loose sand under monotonic shearing”, *Soils and Foundations*, vol. 54, no. 04, pp. 910-916, 2014.
[21] M. Okamura and Y. Soga, “Effects of pore fluid compressibility on liquefaction resistance of partially saturated sand”, *Soils and Foundations*, vol. 46, no. 05, pp. 695-700, 2006.
[22] J. Yang, S. Savidis and M. Roemer M. “Evaluating liquefaction strength of partially saturated sand”, *J Geotech. Geoenviron. Eng*. ASCE vol. 130, no. 09, pp. 975–979, 2004.
[23] K. Ishihara, “Liquefaction and flow failures during earthquakes”, *Geotechnique*, vol. 43, no. 03, pp. 351-415, 1993.
[24] K. Been and M. Jefferies, “A state parameter for sands”, *Geotechnique*, Vol. 35, No. 02, pp. 99-112, 1985.
[25] D. Gallipoli, S.J. Wheeler and M. Karstunen, “Modelling the variation of degree of saturation in a deformable unsaturated soil”, *Geotechnique*, vol. 53, no. 01, pp. 105-112, 2003.